

REFERENCE SIGNAL GENERATION FOR BROADBAND ANC SYSTEMS IN REVERBERANT ROOMS

Fei Ma[†], Wen Zhang^{*†}, and Thushara D. Abhayapala[†]

[†] Research School of Engineering, The Australian National University, Canberra ACT 2601, Australia
{fei.ma, thushara.abhayapala}@anu.edu.au

^{*}Center of Intelligent Acoustics and Immersive Communications,
Northwestern Polytechnical University, Xian 710072, Shaanxi, China
wen.zhang@nwpu.edu.cn

ABSTRACT

One major issue of implementing broadband active noise control systems in reverberant rooms is the lack of reference signals. In this work, by exploiting the spatial sound field characteristics, a time-domain sound field separation method is developed to generate the reference signal for broadband active noise control systems in reverberant rooms. The time-domain sound field separation method separates the outgoing field produced by the primary source from the secondary source feedback and room reverberation on a spherical array, based on spherical harmonic decomposition of the sound field and the radial particle velocity measured by the array. Both the effectiveness of the time-domain sound field separation method and the applicability of the separated outgoing field as the reference signal for a broadband active noise control system in a reverberant room are demonstrated by simulations.

Index Terms— Active noise control, reverberation, sound field separation, spherical harmonics, wave domain

1. INTRODUCTION

A broadband active noise control (ANC) system cancels the primary noise by suppressing it with a secondary noise, which is generated by filtering a reference signal of the primary noise [1]. But the presence of the secondary source feedback and room reverberation makes it difficult to obtain a reference signal of the primary noise for broadband ANC systems implemented in reverberant rooms. For broadband ANC systems in ducts, the reference signal can be generated by removing the secondary source feedback from the reference sensor measurement though the auxiliary-noise-aided online feedback path estimation method [1], [2], [3]. However, the performance of this method is limited in the room environment, where the feedback paths are long and time-varying [3]. To the authors' best knowledge, there is still no effective method to generate the reference signals for broadband ANC systems in reverberant rooms.

In this work, the authors propose to generate the reference signal for broadband ANC systems in reverberant rooms using sound field separation (SFS) methods [4]. The principle is to separate out a signal highly correlated with the primary noise from the secondary source feedback and room reverberation by exploiting the spatial sound field characteristics. Existing frequency-domain and time-domain SFS methods are reviewed in the following paragraph.

Thanks to Australian Research Councils Discovery Projects funding scheme (project no. DP140103412). The work of Fei was sponsored by the China Scholarship Council with the Australian National University.

Given measurements of the sound pressure or the particle velocity on two sensor arrays [5]- [7], or measurements of the sound pressure and the particle velocity together on one sensor array [8]- [10], the frequency-domain methods are able to separate the sound fields originating from two sides of the sensor arrays apart. But the frequency-domain methods introduce additional processing delays, thus do not suit reference signal generation for broadband ANC systems in reverberant rooms, which have strict causal control requirements [1]. Time domain SFS methods are preferred to generate the reference signal for broadband ANC systems. However, existing time-domain methods can only separate apart the sound fields originating from two sides of planar sensor arrays [11], [12], but not necessary the sound produced by the primary source in a broadband ANC system, where intervening sources maybe present around the primary source.

In this work, a time-domain SFS method is developed to generate the reference signal for broadband ANC systems in reverberant rooms. Based on spherical harmonic decomposition of the sound field and the radial particle velocity measured by a spherical array of acoustic vector sensors, the time domain SFS method separates the outgoing field produced by the primary source from the secondary source feedback and room reverberation on the array. The separated outgoing field is used as the reference signal for a broadband ANC system, whose performance is evaluated in a simulated time-varying reverberant room.

2. PROBLEM FORMULATION

Consider a broadband ANC system in a reverberant room as shown in Fig. 1. Let $\mathbf{x} = (x, y, z)$ and $\mathbf{r} = (r, \theta, \phi)$ be the Cartesian coordinates and the spherical coordinates of a point with respect to the origin O , respectively. The broadband ANC system is designed to cancel the primary noise $P_p(t, \mathbf{x}_e)$ produced by the primary source (marked by \blacksquare), by superposing it with the secondary noise $P_s(t, \mathbf{x}_e)$ generated by the secondary sources (marked by \blacklozenge) at two error sensors (marked by \otimes) located at \mathbf{x}_{e_1} and \mathbf{x}_{e_2} .

In a conventional broadband ANC system, a reference sensor would be placed close to the primary source at \mathbf{x}_r . The measurement of the reference sensor is

$$P_r(t, \mathbf{x}_r) = P_p(t, \mathbf{x}_r) + P_s(t, \mathbf{x}_r) + P_\delta(t, \mathbf{x}_r),$$

where $P_p(t, \mathbf{x}_r)$, $P_s(t, \mathbf{x}_r)$, and $P_\delta(t, \mathbf{x}_r)$ are the primary source output, the secondary source feedback, and room reverberation, respectively. The presence of $P_s(t, \mathbf{x}_r)$ and $P_\delta(t, \mathbf{x}_r)$ reduces the coherence between the reference sensor measurement $P_r(t, \mathbf{x}_r)$ and

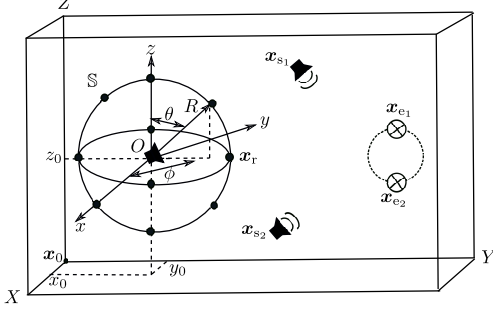


Fig. 1. A broadband ANC system in a reverberant room: The primary source is located at the origin O and marked by \blacksquare , the secondary sources marked by \circ , the error sensors marked by \otimes , the acoustic vector sensors marked by \bullet , and the sphere marked by \mathbb{S} .

the primary noise $P_p(t, \mathbf{x}_e)$ at the error sensor. The performance of the broadband ANC system will deteriorate if the reference sensor measurement is used as the reference signal directly [1], [13].

Denote the sphere of radius R surrounding the primary source as \mathbb{S} , as shown in Fig. 1. The outgoing field on the sphere \mathbb{S} is only generated by the interior sound source, i.e., the primary source, thus is highly correlated with the primary noise $P_e(t, \mathbf{x}_e)$ at the error sensor. The incoming field, on the other hand, is due to the secondary source feedback and room reverberation. In this work, we propose to use a spherical array of acoustic vector sensors (marked by \bullet in Fig. 1) placed on the sphere \mathbb{S} to separate the outgoing field from the incoming field on the sphere \mathbb{S} , and use the separated outgoing field as the reference signal for a broadband ANC system in the reverberant room [14].

3. OUTGOING FIELD SEPARATION ON A SPHERE

In this section, a frequency-domain SFS theory is first reviewed, based on which analytical expressions of a time-domain SFS method are developed. A realization of the method using a spherical array of acoustic vector sensors is presented at the end of this section.

3.1. Review: Frequency-domain theory

In the frequency domain, the sound field $P(k, \Omega)$ on a sphere of radius R can be decomposed as [4], [15], [16]

$$P(k, \Omega) = \sum_{u=0}^{\infty} \sum_{v=-u}^u \alpha_{uv}(k) Y_u^v(\Omega), \quad (1)$$

where $\Omega = (\theta, \phi)$, $k = \omega/c$ is the wave number with c the speed of sound and ω the angular frequency, $Y_u^v(\Omega)$ is the real spherical harmonic of order u and degree v [17], and $\alpha_{uv}(k)$ are the spherical harmonic coefficients. The spherical harmonics in (1) can be truncated to order $N_R = \lceil kR \rceil$, where $\lceil \cdot \rceil$ is the ceiling function [18], [19].

Referring to Sec. 2, the sound field $P(k, \Omega)$ on the sphere \mathbb{S} has two parts, i.e., the outgoing field $P^O(k, \Omega)$ generated by the primary source and the incoming field $P^I(k, \Omega)$ due to the secondary source feedback and room reverberation. Thus, we have [4], [9], [10]

$$P(k, \Omega) = P^O(k, \Omega) + P^I(k, \Omega) \\ \approx \sum_{u=0}^{N_R} \sum_{v=-u}^u \underbrace{[\iota_{uv}(k) \mathcal{H}_u(kR)]}_{\alpha_{uv}^O(k)} + \underbrace{[\kappa_{uv}(k) \mathcal{J}_u(kR)]}_{\alpha_{uv}^I(k)} Y_u^v(\Omega), \quad (2)$$

where $\alpha_{uv}^O(k)$ and $\alpha_{uv}^I(k)$ are the outgoing and incoming field coefficients, respectively. $\mathcal{H}_u(\cdot)$ is the second-kind spherical Hankel function of order u , and $\mathcal{J}_u(\cdot)$ is the first-kind spherical Bessel function of order u .

The frequency-domain radial particle velocity on the sphere \mathbb{S} can be similarly expressed as [4], [9], [10]

$$V(k, \Omega) = \frac{i}{\rho c k} \cdot \frac{\partial P(k, \Omega)}{\partial r} \Big|_{r=R} \approx \sum_{u=0}^{N_R} \sum_{v=-u}^u \beta_{uv}(k) Y_u^v(\Omega) \\ \approx \frac{i}{\rho c} \sum_{u=0}^{N_R} \sum_{v=-u}^u [\iota_{uv}(k) \mathcal{H}'_u(kR) + \kappa_{uv}(k) \mathcal{J}'_u(kR)] Y_u^v(\Omega), \quad (3)$$

where $\beta_{uv}(k)$ are spherical harmonic coefficients corresponding to the radial particle velocity $V(k, \Omega)$ decomposition on the sphere \mathbb{S} . $\mathcal{H}'_u(kR)$ and $\mathcal{J}'_u(kR)$ are differentiations about the argument kR . i is the unit imaginary number, and ρ is the density of air.

From (2) and (3), the frequency-domain outgoing field coefficients $\alpha_{uv}^O(k)$ are obtained as [4], [9]

$$\alpha_{uv}^O(k) = -i(kR)^2 \mathcal{J}'_u(kR) \mathcal{H}_u(kR) \alpha_{uv}(k) \\ + \rho c (kR)^2 \mathcal{J}_u(kR) \mathcal{H}_u(kR) \beta_{uv}(k). \quad (4)$$

Given $\alpha_{uv}^O(k)$, the frequency-domain outgoing field on the sphere \mathbb{S} is expressed as

$$P^O(k, \Omega) \approx \sum_{u=0}^{N_R} \sum_{v=-u}^u \alpha_{uv}^O(k) Y_u^v(\Omega). \quad (5)$$

3.2. Proposed: Time-domain method

The analytical expressions for a time-domain SFS method are shown in the following theorem.

Theorem 1. The time-domain outgoing field $P^O(t, \Omega)$ on the sphere \mathbb{S} of radius R is written as

$$P^O(t, \Omega) \approx \sum_{u=0}^{N_R} \sum_{v=-u}^u \zeta_{uv}^O(t) Y_u^v(\Omega), \quad (6)$$

with coefficients $\zeta_{uv}^O(t)$ given by

$$\zeta_{uv}^O(t) = \int_0^{2\pi} \int_0^\pi Y_u^v(\Omega) \left[\int_0^{2\tau R} h_1^u(\tau) dP(t - \tau, \Omega) \right] d\Omega \\ + \rho c \int_0^{2\pi} \int_0^\pi Y_u^v(\Omega) \left[\int_0^{2\tau R} h_2^u(\tau) dV(t - \tau, \Omega) \right] d\Omega, \quad (7)$$

where $\tau_R = R/c$, and

$$h_1^u(t) = \frac{u}{4} \sum_{v=0}^u \sum_{v'=0}^u \frac{a_v(u) a_{v'}(u)}{(v+v'+1)!} \left[(-1)^v \left(\frac{t}{\tau_R} \right)^{v+v'+1} \text{Sign}(t) \right. \\ \left. + (-1)^{u+1} \left(\frac{t-2\tau_R}{\tau_R} \right)^{v+v'+1} \text{Sign}(t-2\tau_R) \right] \\ + \frac{1}{4} \sum_{v=0}^{u+1} \sum_{v'=0}^u \frac{a_v(u+1) a_{v'}(u)}{(v+v')!} \left[(-1)^v \left(\frac{t}{\tau_R} \right)^{v+v'} \text{Sign}(t) \right. \\ \left. + (-1)^u \left(\frac{t-2\tau_R}{\tau_R} \right)^{v+v'} \text{Sign}(t-2\tau_R) \right], \quad (8)$$

$$h_2^u(t) = \frac{1}{4} \sum_{v=0}^u \sum_{v'=0}^u \frac{a_v(u) a_{v'}(u)}{(v+v')!} \left[(-1)^v \left(\frac{t}{\tau_R} \right)^{v+v'} \text{Sign}(t) \right. \\ \left. + (-1)^{u+1} \left(\frac{t-2\tau_R}{\tau_R} \right)^{v+v'} \text{Sign}(t-2\tau_R) \right], \quad (9)$$

where $\text{Sign}(\cdot)$ is the sign function, and $a_v(u) = \frac{(u+v)!}{2^v v! (u-v)!}$ [20].

Proof. Substitution of k by ω , and R by τ_R in (4) results in

$$\begin{aligned} \alpha_{uv}^O(\omega) &= -\tau_R(\tau_R\omega)\mathcal{J}'_u(\tau_R\omega)\mathcal{H}_u(\tau_R\omega) \times (i\omega)\alpha_{uv}(\omega) \\ &\quad -\rho c\tau_R(\tau_R\omega)\mathcal{J}_u(\tau_R\omega)\mathcal{H}_u(\tau_R\omega) \times (i\omega)\beta_{uv}(\omega). \end{aligned} \quad (10)$$

Then, we define

$$\begin{aligned} \zeta_{uv}^O(t) &= \mathcal{F}^{-1}[\alpha_{uv}^O(\omega)] \\ &= h_1^u(t) * \epsilon_{uv}(t) + \rho c h_2^u(t) * \varepsilon_{uv}(t), \end{aligned} \quad (11)$$

where \mathcal{F}^{-1} denotes the inverse Fourier transform, and the definitions of $h_1^u(t)$, $h_2^u(t)$, $\epsilon_{uv}(t)$, and $\varepsilon_{uv}(t)$ are given in (12)-(15). Here, $\epsilon_{uv}(t)$ and $\varepsilon_{uv}(t)$ are obtained by decomposing the time derivatives of the sound field $P(t, \Omega)$ and the radial particle velocity $V(t, \Omega)$ on the sphere \mathbb{S} into spherical harmonics

$$\begin{aligned} \epsilon_{uv}(t) &= \mathcal{F}^{-1}\left\{(i\omega)\alpha_{uv}(\omega)\right\} \\ &= \frac{d}{dt}\left\{\mathcal{F}^{-1}\left[\int_0^{2\pi}\int_0^\pi P(\omega, \Omega)d\Omega\right]\right\} \\ &= \frac{d}{dt}\left\{\int_0^{2\pi}\int_0^\pi P(t, \Omega)d\Omega\right\} \\ &= \int_0^{2\pi}\int_0^\pi \frac{dP(t, \Omega)}{dt} Y_u^v(\Omega)d\Omega, \end{aligned} \quad (12)$$

$$\begin{aligned} \varepsilon_{uv}(t) &= \mathcal{F}^{-1}\left\{(i\omega)\beta_{uv}(\omega)\right\} \\ &= \frac{d}{dt}\left\{\mathcal{F}^{-1}\left[\int_0^{2\pi}\int_0^\pi V(\omega, \Omega)d\Omega\right]\right\} \\ &= \frac{d}{dt}\left\{\int_0^{2\pi}\int_0^\pi V(t, \Omega)d\Omega\right\} \\ &= \int_0^{2\pi}\int_0^\pi \frac{dV(t, \Omega)}{dt} Y_u^v(\Omega)d\Omega. \end{aligned} \quad (13)$$

Next, based on expressions of the spherical Bessel function and the spherical Hankel function [4], [20]

$$\begin{aligned} \mathcal{H}_u(x) &= e^{-ix} i^{u+2} \sum_{v=0}^u \frac{a_v(u)}{(ix)^{v+1}}, \\ \mathcal{J}_u(x) &= \frac{1}{2}[\mathcal{H}_u(x)^* + \mathcal{H}_u(x)], \\ \mathcal{J}'_u(x) &= \frac{u}{x}\mathcal{J}_u(x) - \mathcal{J}_{u+1}(x), \end{aligned}$$

where $*$ is the complex conjugate operation, we have the following expansions

$$\begin{aligned} h_1^u(t) &= \mathcal{F}^{-1}\left\{-\tau_R(\tau_R\omega)\mathcal{J}'_u(\tau_R\omega)\mathcal{H}_u(\tau_R\omega)\right\} \\ &= \mathcal{F}^{-1}\left\{\frac{u}{2}\sum_{v=0}^u\sum_{v'=0}^u a_v(u)a_{v'}(u)\left[\frac{(-1)^v + e^{-2i\tau_R\omega}(-1)^{u+1}}{\tau_R^{v+v'+1}(i\omega)^{v+v'+2}}\right]\right. \\ &\quad \left. + \frac{1}{2}\sum_{v=0}^{u+1}\sum_{v'=0}^u a_v(u+1)a_{v'}(u)\left[\frac{(-1)^v + e^{-2i\tau_R\omega}(-1)^u}{\tau_R^{v+v'+1}(i\omega)^{v+v'+1}}\right]\right\}, \quad (14) \\ h_2^u(t) &= \mathcal{F}^{-1}\left\{-\tau_R(\tau_R\omega)\mathcal{J}_u(\tau_R\omega)\mathcal{H}_u(\tau_R\omega)\right\} \\ &= \mathcal{F}^{-1}\left\{\frac{\tau_R}{2}\sum_{v=0}^u\sum_{v'=0}^u a_v(u)a_{v'}(u)\right. \\ &\quad \left.\times\left[\frac{(-1)^v + (-1)^{u+1}e^{-i2\omega\tau_R}}{(i\omega\tau_R)^{v+v'+1}}\right]\right\}. \end{aligned} \quad (15)$$

Evaluation of (14) and (15) generates (8) and (9), respectively. Substitution of (12)-(15) into (11) leads to (7). To save space, only the main steps of the proof are shown, and the details will be presented in a future paper. \square

3.3. A realization of the time-domain SFS method

A realization of the time-domain SFS method by a spherical array of acoustic vector sensors is presented here.

Place Q acoustic vector sensors on the sphere \mathbb{S} at $\mathbf{x}_q = (R, \Omega_q)$, with $Q \geq (N_R + 1)^2$ [21]. Replace the continuous integration over the sphere in (7) by a finite summation at Q sampling points with sampling weights $\{\gamma_q\}_{q=1}^Q$. An example is the Gaussian-Legendre sampling scheme [21], which is used in the simulation. And with measurements of the sound pressure $P(n, \Omega_q)$ and the radial particle velocity $V(n, \Omega_q)$ at discrete time instant n , we have

$$\begin{aligned} \zeta_{uv}^O(n) &\approx \sum_{q=1}^Q \gamma_q Y_u^v(\Omega_q) \times \\ &\quad \sum_{n'=0}^{N_0} \left\{ h_1^u(n') [P(n-n', \Omega_q) - P(n-1-n', \Omega_q)] \right. \\ &\quad \left. + \rho c h_2^u(n') [V(n-n', \Omega_q) - V(n-1-n', \Omega_q)] \right\}, \end{aligned} \quad (16)$$

where N_0 is the number of time-domain samples corresponding to $2\tau_R$. The differentiations of the sound pressure and the radial velocity with respect to time are approximated by finite differences. This approximation introduces one sample delay to the time-domain SFS method.

Substitution of $\zeta_{uv}^O(t)$ by $\zeta_{uv}^O(n)$ into (6), results in the outgoing field at an arbitrary point on the sphere \mathbb{S} at discrete time instants.

4. SIMULATION EXAMPLES

Simulation examples in this section illustrate the effectiveness of the time-domain SFS method and its application in generating the reference signal for a broadband ANC system in a reverberant room.

The simulation environment is a rectangular room of size 4 m \times 4.5 m \times 5 m as shown in Fig. 1. The wall reflection coefficients are [0.71, 0.72, 0.74, 0.76, 0.78, 0.8]. One corner of the room is located at $\mathbf{x}_0 = (-1.5, -2.0, -1.8)$ m with respect to the origin O . The radius of the sphere \mathbb{S} is $R = 0.34$ m. The speed of sound is $c = 343$ m/s, and the air density is $\rho = 1.225$ kg/m³. The room impulse responses (including the radial partial velocity response) are 6800 taps long and simulated using the image source method [22]. The sampling frequency is $f_s = 34$ kHz. N_0 in (16) is chosen based on $\lceil 2R/c \times f_s \rceil + 1 = 69$. At each sensor output, thermal noise is added such that the signal-to-noise ratio is 30 dB. The adaptive filter coefficients are initialized as zeros, and the step-size parameters are chosen by trial-and-error. The simulation results are from an average of 100 independent runs. The settings presented in this paragraph are used in the simulations unless otherwise stated.

Two simulations are conducted and the first simulation is about time-domain SFS. We place three point sources at (0.25, 0.0, 0.1) m, (0.0, -0.24, 0.0) m, and (-0.1, 0.0, -0.2) m inside of the sphere \mathbb{S} , and three point sources at (0.0, -0.51, 0.0) m, (-0.3, 1.0, 0.0) m, and (-0.5, 0.0, 0.5) m outside of the sphere \mathbb{S} . The outputs of the sources are of the form $\sum_{s=1}^6 \sum_{l=0}^{100} a_{s,l} \cos(2\pi(f_0 + \Delta_f \times l)n)$, where $f_0 = 100$ Hz, $\Delta_f = 5$ Hz, and the amplitudes $\{a_{s,l}\}$ are drawn from a zero-mean unit-variance Gaussian sequence. The truncation order is $N_R = 5$ [18], [19]. A spherical array of 72 acoustic vector sensors are placed on the sphere \mathbb{S} according to the Gauss-Legendre sampling scheme [21]. We perform SFS on the sphere for $T = 30$ ms. Figure 2 depicts at time instant $n = 23.5$ ms the amplitudes of the outgoing field $P^O(n, \Omega)$, the total field $P(n, \Omega)$,

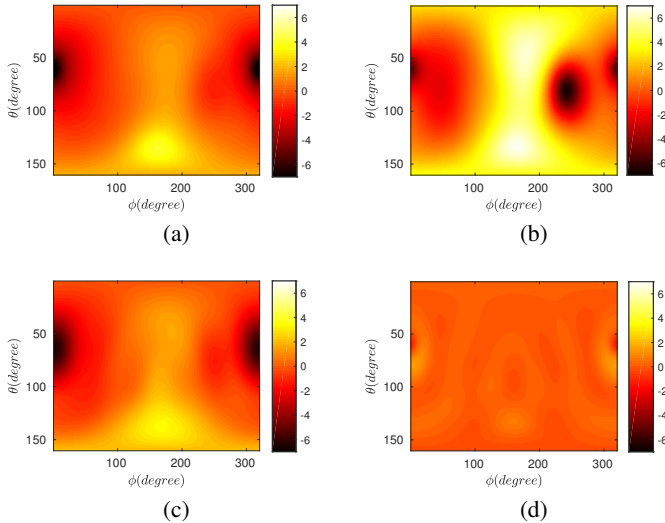


Fig. 2. At time instant $n = 23.5$ ms the amplitudes of the outgoing field (a), the total field (b), the separated outgoing field (c), and the field separation error (d) on the sphere \mathbb{S} .

the separated outgoing field $\hat{P}^O(n, \Omega)$, and the field separation error $P_e^O(n, \Omega) = P^O(n, \Omega) - \hat{P}^O(n, \Omega)$ on the sphere \mathbb{S} at $\Gamma = 160 \times 320$ equal-angle sampling points [21]. As shown in Fig. 2, the time-domain SFS method can accurately separate out the outgoing field on the sphere \mathbb{S} . And the outgoing field separation error over the period and over the sphere is

$$\varsigma = 10 \log_{10} \frac{\sum_{n=0}^T \sum_{q=1}^{\Gamma} \|P_e^O(n, \Omega_q)\|^2}{\sum_{n=0}^T \sum_{q=1}^{\Gamma} \|P^O(n, \Omega_q)\|^2} = -19.4 \text{ dB}.$$

The second simulation is about noise cancellation. As shown in Fig. 1, a primary source is placed at the origin O , and two secondary sources are placed at $(\pm 0.75, 0.75, 0.0)$ m. The primary source generates a broadband noise same as in the first simulation. We propose an ANC system that uses the time-domain SFS method to generate a reference signal, and compare its performance with the conventional ANC system in [3]. These two ANC systems are designed to reduce the noises at two error sensors located at $(\pm 0.09, 2.0, 0.0)$ m.

In the proposed ANC system, a spherical array with 32 acoustic vector sensors are placed on the sphere \mathbb{S} according to the Gauss-Legendre sampling scheme [21]. The truncation order is $N_R = 3$ [18], [19]. The outgoing field separated by the time-domain SFS method at the 13-th acoustic vector sensor is used as the reference signal. For the conventional ANC system, the sound pressure measured by a reference sensor located at $\mathbf{x}_r = (-0.32, 0.0, 0.15)$ m, is processed by a feedback path modeling and neutralization (FBPMN) filter, and the resulting signal is used as the reference signal [3]. The sub-filters of the FBPMN filter are all 6800 taps long with two step-size parameters $\mu_h = 1 \times 10^{-4}$ and $\mu_f = 2.5 \times 10^{-5}$ [3]. The FBPMN filter uses two white noises to model the feedback paths, and the white noise to the primary noise power ratios at error sensors are -20 dB. The coefficients of the feedback path modeling sub-filter in the FBPMN filter are initialized as the coefficients of the true feedback path [3].

The secondary source outputs of the proposed and conventional systems are generated by passing the corresponding reference signals through two 6800-tap filters, whose coefficients are updated by

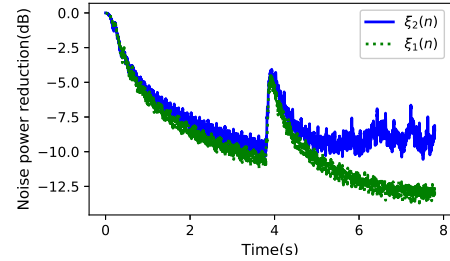


Fig. 3. Noise power reduction at Sensor 1 achieved by the proposed system $\xi_1(n)$, and by the conventional system $\xi_2(n)$.

the multiple error least-mean-square algorithm with step-size parameter $\mu_w = 1 \times 10^{-4}$ [23]. The secondary paths have 6800 coefficients and are known by both two systems.

Denote the noise power reduction at the error sensor as

$$\xi(n) = 10 \log_{10} (\|P_e(n)\|^2 / \|P_p^2(n)\|^2),$$

where $P_p(n)$ and $P_e(n)$ are the primary noise and residual noise at the error sensor at time n , respectively. Figure 3 depicts noise power reduction at Sensor 1, i.e., $(-0.09, 2.0, 0.0)$ m, achieved by the proposed system $\xi_1(n)$, and by the conventional system $\xi_2(n)$. Noise power reduction at Sensor 2 shows similar trends, thus is not shown to save space. At time $n = 4$ s, the wall reflection coefficients are increased from $[0.71, 0.72, 0.74, 0.76, 0.78, 0.8]$ to $[0.9, 0.9, 0.9, 0.9, 0.9, 0.9]$ to simulate a time-varying acoustic environment. The increase of the reflection coefficients causes the feedback path coefficients change abruptly. As shown in Fig. 3, the noise power reduction achieved by the conventional system is slightly worse than the proposed system before $n = 4$ s. That's because, the white noises injected by the conventional system increase the noise pressure levels at the error sensors. After that, the performance of the conventional system deteriorates, because the FBPMN filter fails to track the feedback path changes, and unable to provide a reference signal correlated with the primary noise. The performance of the proposed system is not affected by the feedback path changes. At $n = 8$ s, the noise power at Sensor 1 is reduced by the proposed system by more than 12.5 dB. Using variable step-size parameters or auxiliary-noise power scheduling method can improve the performance of the FBPMN filter, but that will make the conventional system complicated [24], [25]. On the other hand, the proposed ANC system, relying on the time-domain SFS method, is easy to implement.

5. CONCLUSION

In this paper, we explored SFS methods to generate reference signals for broadband ANC systems in reverberant rooms. Based on spherical harmonic decomposition of the sound field and the radial particle velocity measured by a spherical array enclosing the primary source, a time-domain SFS method was developed to separate the outgoing field produced by the primary source from the secondary source feedback and room reverberation on the array. In simulations, using the separated outgoing field as the reference signal, the proposed broadband ANC system demonstrated robust noise cancellation performance in a time-varying reverberant room. Apart from generating a reference signal for a broadband ANC system, the time-domain SFS method can also be used for monitoring the working condition of a machine, and for speech dereverberation [5], [7].

6. REFERENCES

- [1] S. M. Kuo and D. R. Morgan, *Active noise control systems: algorithms and DSP implementations*, New York: Wiley, 1995.
- [2] M. T. Akhtar, M. Abe, and M. Kawamata, "On active noise control systems with online acoustic feedback path modeling," *IEEE Trans. Audio Speech Lang. Process.*, vol. 15, no. 2, pp. 593–600, Feb. 2007.
- [3] M. T. Akhtar, M. Abe, M. Kawamata, and W. Mitsuhashi, "A simplified method for online acoustic feedback path modeling in multichannel active noise control systems," in *SICE Annual Conference*, Aug. 2008, pp. 50–54.
- [4] E. G. Williams, *Fourier acoustics: sound radiation and nearfield acoustical holography*, New York: Academic, 1999.
- [5] L. Christophe, M. Manuel, and G. Alexandre, "Boundary element method for the acoustic characterization of a machine in bounded noisy environment," *J. Acoust. Soc. Am.*, vol. 121, no. 5, pp. 2750–2757, 2007.
- [6] C. Bi, X. Chen, and J. Chen, "Sound field separation technique based on equivalent source method and its application in nearfield acoustic holography," *J. Acoust. Soc. Am.*, vol. 123, no. 3, pp. 1472–1478, 2008.
- [7] A. Fahim, P. N. Samarasinghe, and T. D. Abhayapala, "Extraction of exterior field from a mixed sound field for 2d height-invariant sound propagation," in *2016 International Workshop on Acoustic Signal Enhancement (IWAENC)*, IEEE, pp. 1–5.
- [8] E. Fernandez-Grande and F. Jacobsen, "Sound field separation with sound pressure and particle velocity measurements," *J. Acoust. Soc. Am.*, vol. 132, no. 6, pp. 3818–3825, 2012.
- [9] M. Melon, C. Langrenne, P. Herzog, and A. Garcia, "Evaluation of a method for the measurement of subwoofers in usual rooms," *J. Acoust. Soc. Am.*, vol. 127, no. 1, pp. 256–263, 2010.
- [10] Y. Braikia, M. Melon, C. Langrenne, E. Bavu, and A. Garcia, "Evaluation of a separation method for source identification in small spaces," *J. Acoust. Soc. Am.*, vol. 134, no. 1, pp. 323–331, 2013.
- [11] X. Zhang, J. H. Thomas, C. Bi, and J. C. Pascal, "Separation of nonstationary sound fields in the time-wavenumber domain," *J. Acoust. Soc. Am.*, vol. 131, no. 3, pp. 2180–2189, 2012.
- [12] C. Bi, L. Geng, and X. Zhang, "Separation of non-stationary sound fields with a single layer pressure-velocity measurements," *J. Acoust. Soc. Am.*, vol. 139, no. 2, pp. 781–789, 2016.
- [13] B. Rafaely, "Zones of quiet in a broadband diffuse sound field," *J. Acoust. Soc. Am.*, vol. 110, no. 1, pp. 296–302, 2001.
- [14] H. E. de Bree, "The microflow: An acoustic particle velocity sensor," *Acoust. Aust.*, vol. 31, no. 3, pp. 91–94, 2003.
- [15] T. D. Abhayapala, "Modal analysis and synthesis of broadband nearfield beamforming arrays", Ph.D. dissertation, Australian Nat. Univ., Canberra, Australia, 1999.
- [16] M. A. Poletti, T. D. Abhayapala, and P. D. Teal, "Time domain description of spatial modes of 2D and 3D free-space greens functions," in *Audio Engineering Society Conference: 2016 AES International Conference on Sound Field Control*, Audio Engineering Society, 2016.
- [17] M. A. Poletti, "Unified description of ambisonics using real and complex spherical harmonics," *Proc. Ambisonics Symp.*, 2009, pp. 1–10.
- [18] D. B. Ward and T. D. Abhayapala, "Reproduction of a plane-wave sound field using an array of loudspeakers," *IEEE Trans. Speech Audio Process.*, vol. 9, no. 6, pp. 697–707, 2001.
- [19] S. Brown, S. Wang, and D. Sen, "Analysis of the spherical wave truncation error for spherical harmonic soundfield expansions," in *IEEE International Conference on Acoustics, Speech and Signal Processing (ICASSP)*, March 2012, pp. 5–8.
- [20] F. W. J. Olver, A. B. Olde Daalhuis, D. W. Lozier, B. I. Schneider, R. F. Boisvert, C. W. Clark, B. R. Miller, and B. V. Saunders, eds, "*NIST Digital Library of Mathematical Functions*," <http://dlmf.nist.gov/>, Release 1.0.15 of 2017-06-01.
- [21] B. Rafaely, *Fundamentals of Spherical Array Processing*, vol. 8, Springer, 2015.
- [22] J. B. Allen and D. A. Berkley, "Image method for efficiently simulating small-room acoustics," *J. Acoust. Soc. Am.*, vol. 65, no. 4, pp. 943–950, 1979.
- [23] S. J. Elliott, I. Stothers, and P. A. Nelson, "A multiple error LMS algorithm and its application to the active control of sound and vibration," *IEEE Trans. Acoust. Speech Signal Process.*, vol. 35, no. 10, pp. 1423–1434, Oct. 1987.
- [24] M. T. Akhtar and W. Mitsuhashi, "Variable step-size based method for acoustic feedback modeling and neutralization in active noise control systems," *Appl. Acoust. Audio, and Signal Process.*, vol. 72, no. 5, pp. 297–304, Apr. 2011.
- [25] S. Ahmed, M. T. Akhtar, and X. Zhang, "Online acoustic feedback mitigation with improved noise-reduction performance in active noise control systems," *IET Signal Process.*, vol. 7, no. 6, pp. 505–514, Aug. 2013.